The Astrophysical Journal Letters, 833:L9 (5pp), 2016 December 10 doi:10.3847/2041-8213/833/1/L9


# WHAT IS EATING OZONE? THERMAL REACTIONS BETWEEN $SO_2$ AND $O_3$: IMPLICATIONS FOR ICY ENVIRONMENTS

Mark J. Loeffler and Reggie L. Hudson
NASA Goddard Space Flight Center, Astrochemistry Laboratory, Code 691, Greenbelt, MD 20771, USA; mark.loeffler@nasa.gov
*Received 2016 October 17; revised 2016 November 15; accepted 2016 November 15; published 2016 December 5*

## ABSTRACT

Laboratory studies are presented, showing for the first time that thermally driven reactions in solid $H_2O + SO_2 + O_3$ mixtures can occur below 150 K, with the main sulfur-containing product being bisulfate ($HSO_4^-$). Using a technique not previously applied to the low-temperature kinetics of either interstellar or solar-system ice analogs, we estimate an activation energy of 32 kJ $mol^{-1}$ for $HSO_4^-$ formation. These results show that at the temperatures of the Jovian satellites, $SO_2$ and $O_3$ will efficiently react making detection of these molecules in the same vicinity unlikely. Our results also explain why $O_3$ has not been detected on Callisto and why the $SO_2$ concentration on Callisto appears to be highest on that world's leading hemisphere. Furthermore, our results predict that the $SO_2$ concentration on Ganymede will be lowest in the trailing hemisphere, where the concentration of $O_3$ is the highest. Our work suggests that thermal reactions in ices play a much more important role in surface and sub-surface chemistry than generally appreciated, possibly explaining the low abundance of sulfur-containing molecules and the lack of ozone observed in comets and interstellar ices.

*Key words:* astrochemistry – comets: general – evolution – methods: laboratory: solid state – planets and satellites: surfaces – radiation mechanisms: thermal

## 1. INTRODUCTION

It is well known that ionizing radiation incident on the Jovian satellites can induce chemical changes in surface ices, but the role of low-temperature thermally induced chemistry has rarely been explored. In recent years, we have investigated bisulfite ($HSO_3^-$) formation from the reaction of $SO_2$ with $H_2O$ at ~70 – 130 K (Loeffler & Hudson 2010), with a subsequent conversion to sulfate ($SO_4^{2-}$) in the presence of radiolytically generated $H_2O_2$ (Loeffler & Hudson 2013). However, the possibility that similar reactions might occur with other oxidants, on icy satellites, or in cometary or interstellar ices has yet to be addressed and answered. Here, we describe a second case of thermally induced oxidation, with ozone ($O_3$) instead of $H_2O_2$ as the oxidizing agent. We use this discovery to argue that thermal reactions can help explain both the observed hemispherical compositional differences on icy satellites and the lack of $O_3$ detections in comets and interstellar ices. We conclude (1) that such reactions in ices can play a much more important role in surface and sub-surface chemistry than is generally appreciated, and (2) that they might help resolve the discrepancy between the ease with which $O_3$ is made in laboratory cosmic-ice analogs and the rarity with which it is observed in interstellar and planetary environments.

The detection of ozone ($O_3$) on Ganymede, Rhea, and Dione (Noll et al. 1997), through the ozone's strong uv absorption near 260 nm, shows that radiation chemistry alters the composition of the surface of each of these worlds. Given that these surfaces are composed predominately of $H_2O$-ice, from which ozone can be produced from the $O_2$ made by radiolysis of $H_2O$, it is somewhat surprising that other icy satellites have not shown evidence of solid $O_3$. While there are environmental differences among icy satellites, none readily explain why Ganymede, Rhea, and Dione are the only objects where solid ozone is present.

Noll et al. (1997) noted that one reason for the lack of additional $O_3$ detections is that other molecules, such as $SO_2$, might compete for O atoms produced via radiolysis of the surface $H_2O$-ice. This possible anti-correlation between two molecules, $SO_2$ and $O_3$, is similar to what has been observed on Europa, where $SO_2$ and $H_2O_2$, another product of $H_2O$ radiolysis, are largely confined to different hemispheres (Domingue & Lane 1998; Carlson et al. 1999; Hendrix et al. 2011). Through laboratory studies, our group showed that under relevant Europa conditions, $SO_2$ and $H_2O_2$ indeed react via thermally driven reactions on very short timescales (Loeffler & Hudson 2013), supporting previous observations and suggesting that at the temperatures of the icy satellites, these two molecules will not be found in the same vicinity. Furthermore, our observation that such reactions readily occur at temperatures of the icy satellites (~100 K) without the need of an external energy source underscores the importance of non-radiolytic reactions for not only surface-ice chemistry, but also for processing sub-surface ices.

Given the propensity of $SO_2$ to react in $H_2O + H_2O_2$ ices, we now report that thermally driven reactions also occur in $H_2O + SO_2 + O_3$ ices. In the following, we describe how infrared (IR) spectroscopy was used to both identify the main reaction products and to estimate the reaction's activation energy.

## 2. EXPERIMENTAL

The experimental setup, equipment, and procedures to prepare our ices and to quantify our results have been described previously (Loeffler & Hudson 2010, 2013). To make pure $O_3$ we filled a glass manifold with ~100 Torr of $O_2$ and sparked it with a Tesla coil discharge for ~15 minutes. During this time, part of the manifold was immersed in liquid nitrogen to collect the $O_3$ product. After the discharge was turned off, the remaining $O_2$ was pumped away, leaving the liquid $O_3$ behind.

The $H_2O + SO_2 + O_3$ (76:21:3) ices used in this study had a thickness of 1.4 ± 0.1 $\mu$m, assuming that the density of $O_3$ is 1.73 g $cm^{-3}$ (Streng & Grosse 1959) and the refractive index at

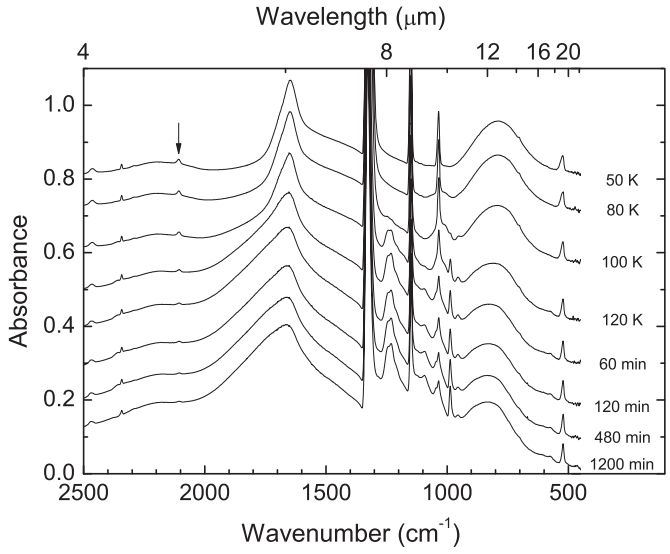


**Figure 1.** Evolution of a $H_2O + SO_2 + O_3$ sample (76:21:3) during heating to and annealing at 120 K. The bottom four spectra are labeled by the time elapsed after the sample had reached 120 K. The vertical arrow highlights the 2108 $cm^{-1}$ $O_3$ band used for analysis.

670 nm is 1.50. We estimated the refractive index by applying the Lorentz–Lorenz approximation (Lorentz 1880; Lorenz 1881) using the published values for density and molar refractivity (Maryott and Buckley 1953). As we have done previously, we characterized our samples using infrared spectroscopy; details can be found in Loeffler & Hudson (2013).

To quantify the loss of ozone in our samples, we matched the baseline of ozone's 2108 $cm^{-1}$ overtone absorption with a straight line and then integrated this same $O_3$ IR feature; we did not integrate the fundamental vibrational band at 1040 $cm^{-1}$ because multiple products absorbed in this region, complicating the analysis. As both pure $O_3$ and pure $SO_2$ sublimate at the higher temperatures used in this study, we performed control experiments to check the possibility of thermal loss contributing to the absorption. We found that a low concentration of $O_3$ was thermally stable overnight in a $H_2O + O_3$ sample at 130 K. Furthermore, we also observed that between 50 and 130 K, the strength of the 2108 $cm^{-1}$ ozone absorption band decreased nearly linearly by ∼15%, an observation we used in our calculations.

## 3. RESULTS

The IR spectra of an $H_2O + SO_2 + O_3$ (76:21:3) ice made by co-deposition of its components at 50 K, during warming to 120 K at 1 K $minute^{-1}$, and while holding at 120 K are shown in Figure 1. After deposition, each compound was easily identified in the 2500 – 500 $cm^{-1}$ spectral region: $O_3$ (1035 and 2108 $cm^{-1}$), $H_2O$ (1648 and 790 $cm^{-1}$), and $SO_2$ (2463, 1318, 1149, and 523 $cm^{-1}$). On warming to 80 K, spectral changes included the appearance of a new absorption at 954 $cm^{-1}$, the appearance of a broad shoulder under the main ozone absorption (∼1047 $cm^{-1}$), and a broadening on the high-wavenumber side of the $H_2O$ band at 1649 $cm^{-1}$. By ∼100 K, the $O_3$ absorption began to decrease, which coincided with the growth of several new bands. The first identifiable new band was centered near 1230 $cm^{-1}$, with some structure to indicate that it might be a combination of multiple absorptions.

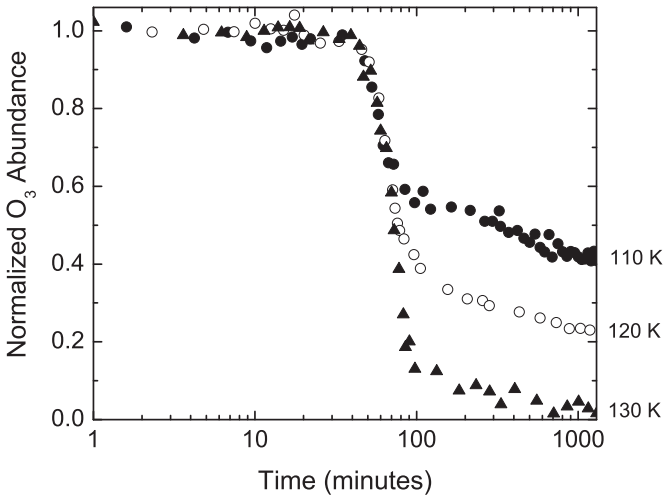


**Figure 2.** Decrease in the area of the 2108 $cm^{-1}$ absorption band in a $H_2O + SO_2 + O_3$ sample (76:21:3) during heating and holding at 110, 120, and 130 K. All samples were deposited at 50 K and warmed at 1 K $minute^{-1}$.

Seemingly corresponding to the growth of the 1230 $cm^{-1}$ feature were other, slightly weaker, absorptions at 573, 987, and 1090 $cm^{-1}$, which also continued to grow as the temperature increased.

Figure 2 shows the $O_3$ abundance in the sample on warming to and holding at 110, 120, and 130 K. In each experiment, the $O_3$ abundance started to decrease near 100 K and continued decreasing as the sample was held at a constant temperature. For the samples at 110 and 120 K, the $O_3$ abundance fell by a factor of 2.5 and a factor of 5.0 after 1200 minutes, while it decreased by a factor of 10 in ∼20 minutes when the sample was held at 130 K.

## 4. DISCUSSION

### 4.1. Reaction Chemistry and Spectral Assignments

To identify the likely reaction sequence observed in our experiments, one can look into work focused on thermal reactions between $SO_2$ and $O_3$ under conditions relevant to Earth's atmosphere (Erickson et al. 1977; Hoffmann 1986; Penkett et al. 1979). In those studies, the reaction sequence is thought to begin with the formation of $HSO_3^-$ via

$$2H_2O + SO_2 \rightarrow HSO_3^- + H_3O^+. \quad (1)$$

In samples where the bisulfate concentration is sufficiently high, $S_2O_5^{2-}$ can form through

$$2HSO_3^- \rightarrow S_2O_5^{2-} + H_2O. \quad (2)$$

These thermal reactions are evident in the first few spectra shown in Figure 1 for our $H_2O + SO_2 + O_3$ ices. For instance, the broad shoulder near 1047 $cm^{-1}$ is due to $HSO_3^-$, the absorption band at 954 $cm^{-1}$ is from $S_2O_5^{2-}$, and the broadening of the $H_2O$ absorption at 1648 $cm^{-1}$ is indicative of $H_3O^+$.

Studies of $SO_2$ and $O_3$ in aqueous solutions found that the bisulfite from (1) was rapidly oxidized to form the bisulfate ($HSO_4^-$) ion (Erickson et al. 1977):

$$O_3 + HSO_3^- \rightarrow HSO_4^- + O_2. \quad (3)$$

Figure 1 shows evidence of reaction (3) beginning near 100 K and continuing as the temperature increased, where the loss of

$O_3$ coincided with an increase in the large absorption band near 1230 $cm^{-1}$, as well as smaller ones at 1090, 987, and 573 $cm^{-1}$, all of which are attributed to bisulfate. We point out that the absorption near 1230 $cm^{-1}$, as well as the weaker one at 1090 $cm^{-1}$, are shifted by ~40 $cm^{-1}$ compared to absorptions in room temperature aqueous solutions of 80 wt% $H_2SO_4$ (Walrafen & Dodd 1961), yet given the difference in environment this size of shift is not unreasonable. That the 1090 and 987 $cm^{-1}$ absorptions could be from another ion, such as sulfate, which absorbs near each of these bands (Loeffler & Hudson 2013), seems unlikely given reaction (3) and that the band near 987 $cm^{-1}$ should be much weaker than the 1090 $cm^{-1}$ sulfate absorption, but yet it is comparable or even stronger in this ice's spectrum. Furthermore, although our sample is an amorphous solid, the 987 and 573 $cm^{-1}$ absorptions also are observed in IR spectra of sulfuric acid monohydrate (Loeffler et al. 2011), a crystalline solid made of $H_3O^+$ and $HSO_4^-$ (Taesler & Olovsson 1968).

### 4.2. Kinetics

As indicated in Figures 1 and 2, it is clear that a reaction consuming $O_3$ occurred in our $H_2O + SO_2 + O_3$ ice and that more $O_3$ was consumed as the temperature was increased. Although this temperature range over which $O_3$ reacted is also found on the Jovian icy satellites, it is of interest to estimate how fast this reaction will occur at lower temperatures where it cannot readily be studied on laboratory timescales. Such estimates require the reaction's activation energy, yet measuring this quantity accurately for solids is typically much more difficult than for gas- or liquid-phase solutions because of the severely limited motion in solid solutions and the distribution in alignments of potential reactants in amorphous solids, such as our ices. Nonetheless, starting with the assumption of a single-step reaction, we write

$$\frac{d\alpha}{dt} = k(T) f(\alpha), \tag{4}$$

where $\alpha$ is the fraction of $O_3$ reacted in time $t$, $k(T)$ is the reaction's rate constant at temperature $T$, and $f(\alpha)$ is the reaction model (Vyazovkin 1996). The main uncertainty in this approach is the selection of $f(\alpha)$, as the estimated activation energy can depend substantially on the selected model (see review by Vyazovkin & Wight 1997). As an alternative to this procedure, we adopt an approach known as the isoconversional method (Vyazovkin 1996), which allows one to calculate an activation energy without relying on $f(\alpha)$. Instead of the usual monitoring of a reaction at temperature $T$, this approach involves following a reaction subjected to a specific warming rate. We believe that this is the first time this method has been used to study the low-temperature kinetics of either interstellar or solar-system ice analogs.

To use the isoconversional method, we first rewrite (4) as

$$\frac{d\alpha}{dT} = \left(\frac{A}{\beta}\right) e^{-E/RT} f(\alpha), \tag{5}$$

where $\beta$ is the heating rate, $E$ is the reaction's activation energy, and $A$ is the usual pre-exponential factor. Next, we take the natural log of both sides and add the subscripts $\alpha$ and $i$ to the relevant dependent terms:

$$\ln\left[\beta_i \left(\frac{d\alpha}{dT}\right)_{\alpha,i}\right] = \ln\left[A_\alpha f(\alpha)\right] - E_\alpha / RT_{\alpha,i}. \tag{6}$$

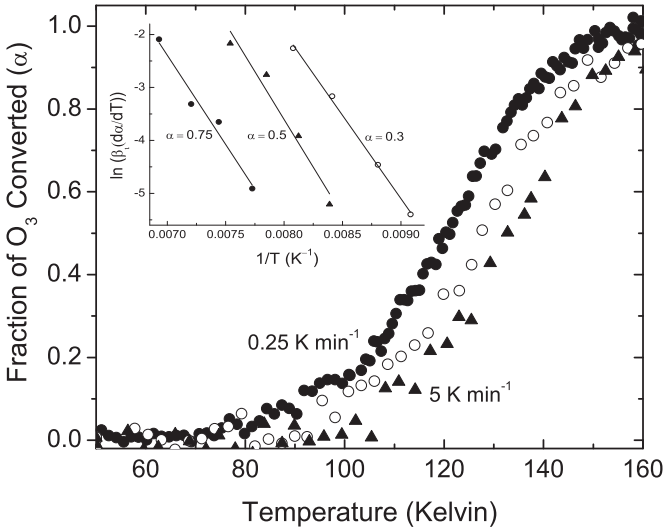


**Figure 3.** Fraction of $O_3$ converted vs. temperature for three different heating rates (K $minute^{-1}$): 0.25 (•), 2.5 (○), and 5 (▲). Inset: three fractions (0.3, 0.5, and 0.75) where Equation (6) was used to calculate the activation energy.

To use (6), we performed experiments at different heating rates ($\beta_i$) between 0.25 and 5 K $minute^{-1}$; three such experiments are shown in Figure 3, where we have plotted $\alpha$ as a function of temperature in the main panel. As in Figure 2, there is little to no change in the $O_3$ abundance below 80 K. However, for the lowest heating rates $\alpha$ begins to change between 80 and 100 K. In all cases, the rate of conversion increases above 100 K and more than 90% of the $O_3$ is converted between 140 and 150 K, depending on the heating rate. Finally, we note that the trend above ~80 K observed in Figure 3 is that the fraction ($\alpha$) of $O_3$ consumed is largest for the slowest heating rate, a reflection of the fact that a slow heating rate translates into a longer reaction time.

To obtain an activation energy, we measured both $\frac{d\alpha}{dT}$ and $\frac{1}{T}$ at a single $\alpha$ for each of the curves shown in Figure 3, in a manner similar to that described by Ozawa (1965) and Flynn & Wall (1966). We estimated $\frac{d\alpha}{dT}$ by applying a linear fit to the data in close proximity to the $\alpha$ value in question. The inset of Figure 3 shows a plot of the left side of (6) versus $\frac{1}{T}$ for the cases of $\alpha = 0.3$, 0.5, and 0.75, with the slope of each line corresponding to $\frac{-E_\alpha}{R}$. Although it is possible that the activation energy is lower in the initial part of the reaction, we estimate $E_\alpha$ to be $32 \pm 5$ kJ $mol^{-1}$ for $0.3 \leqslant \alpha \leqslant 0.8$, where the error given is obtained from the uncertainty of the linear fit used to determine $\frac{-E_\alpha}{R}$. This value is somewhat lower than that for reactions involving $H_2O + SO_2 + H_2O_2$ chemistry (53 kJ $mol^{-1}$), although a simpler approach was used there to determine the activation energy (Loeffler & Hudson 2013). The activation energy reported by Hoffmann (1986) for the $O_3 + HSO_3^-$ reaction in aqueous solution near room temperature is 46 kJ $mol^{-1}$, which is higher than what we measured in our ices. However, given the substantial differences in our conditions and his, we cannot say much more about these two

sets of data, except that $E_\alpha = 32 \pm 5\,\mathrm{kJ\,mol^{-1}}$ appears reasonable.

One goal of kinetic analysis is to enable the extrapolation of laboratory data to estimate reaction times at temperatures where laboratory experiments are not feasible. As with deriving an activation energy, these extrapolations become much less certain as one moves away from the temperatures of the laboratory measurements. For isoconversional methods, one can calculate the time that a certain amount of material would take to react at another temperature using

$$t_\alpha = \left[\beta e^{-\frac{E_\alpha}{RT_0}}\right]^{-1} \int_0^{T_\alpha} e^{-\frac{E_\alpha}{RT}} dT, \quad (7)$$

where $T_\alpha$ is the temperature where $\alpha$ is reached at the specified heating rate and $T_0$ is the temperature to which one is extrapolating (Vyazovkin 1996). Estimates with Equation (7) in the present case give ~200 years for half of the $O_3$ in our ice to be consumed at 80 K and about 5500 years for 80% of the ozone to be converted into bisulfate. In the higher temperature regions of the icy satellites, $O_3$ would be consumed much more rapidly. For instance, one can use Equation (7) to estimate that 80% of the ozone would be converted in less than a minute, which is roughly consistent with our laboratory studies. These times are much shorter than what is needed to produce an observable amount of either $SO_2$, considering the $S^+$ flux irradiating the Galilean icy-satellite surfaces (Cooper et al. 2001), or $O_3$, based on estimates of the time to reach equilibrium via radiolysis with heavy ions at the warmer temperatures of Ganymede (Noll et al. 1996).

### 4.3. Implications for Ice Chemistry

Our experiments show that the $O_3$ abundance on any $H_2O$-rich icy satellite will depend on the $SO_2$ abundance, and vice versa. These results may be particularly relevant for Ganymede, Callisto, and Europa, where solid ozone, or its likely precursor solid $O_2$, and sulfur compounds are suspected to be mixed in surface ices. Thus, below we discuss observations of these icy satellites in light of our new results.

Ganymede's $O_3$ abundance is greatest on its trailing side (Noll et al. 1996), which is consistent with observations there of condensed $O_2$ (Spencer et al. 1995; Calvin et al. 1996) and with the preferential bombardment by magnetospheric ions (Johnson et al. 2004). $SO_2$ has been identified on Ganymede through its 4.05 $\mu$m (2469 $\mathrm{cm^{-1}}$) absorption band (McCord et al. 1998a) but there is little information on whether $SO_2$ is uniformly distributed, likely due to the low abundance observed. Our results suggest that $SO_2$ will be more abundant on the leading hemisphere if it is mixed with the $H_2O$-ice. It is noted that one study observed a possible spectral feature at 320 nm, which was attributed to $SO_2$ frost, rather than $SO_2$ mixed in $H_2O$ (Domingue et al. 1998). This feature was transient in the trailing hemisphere, but absent in the leading hemisphere. As $H_2O$ is required to form the bisulfite that reacts with the $O_3$ in reaction (3), pure $SO_2$ frost could remain stable on an icy satellite's surface.

No $O_3$ has been detected on Callisto, although condensed $O_2$ has been identified in the trailing hemisphere (Spencer & Calvin 2002). This observation is counter to what is expected based on laboratory studies showing $O_3$ is easily formed from radiolysis of solid $O_2$ (Lacombe et al. 1997; Baragiola et al. 1999; Famá et al. 2002). Equally puzzling is the observation that $SO_2$ appears to be more abundant on the leading side of Callisto (McCord et al. 1998b; Hibbitts et al. 2000), which is opposite of what would be expected if $SO_2$ was created by magnetospheric bombardment. We note that there are alternatives to the $SO_2$ assignment on Callisto, such as $H_2CO_3$ or other carbonates (Johnson et al. 2004). However, in light of our laboratory results, it is plausible that both the lack of detection of $O_3$ and lower abundance of $SO_2$ in the Callisto's trailing hemisphere are a result of reaction (3).

On Europa, $O_2$ is present on both hemispheres (Spencer & Calvin 2002), yet no $O_3$ has been detected on either. The presence of $O_3$ on the trailing side is not expected given that $SO_2$ appears to be largely confined to this region (Lane et al. 1981; Domingue & Lane 1998; Hansen & McCord 2008; Hendrix & Johnson 2008; Hendrix et al. 2011). However, the absence of $O_3$ on the leading hemisphere, where $SO_2$ is not nearly as prevalent and even possibly absent (Hendrix et al. 2011), suggests that another compound may react with the ozone or that another process limiting production of ozone may be important.

Although our experiments were designed to probe icy-satellite chemistry, extensions to cometary and interstellar ices are possible. For example, the *Rosetta* mission's ROSINA-DFMS mass spectrometer detected $O_2$ at the level of about 4% relative to $H_2O$ in the coma of comet 67P/Churyumov–Gerasimenko (Bieler et al. 2015), but no $O_3$ was found. Sulfur dioxide ($SO_2$) is a known cometary molecule and will react with $H_2O$-ice to make $HSO_3^-$, and the latter's low-temperature reaction with $O_3$ will lower the abundance of both $HSO_3^-$ and $O_3$. If such reactions do not occur before a comet's passage around the Sun, then they will take place during it, when nuclear ices are warmed and coma material released. A second possible application of the results presented here concerns interstellar ices and their laboratory counterparts. Both radiolysis and photolysis of interstellar-ice analogs containing $CO_2$ readily produce detectable $O_3$. However, $O_3$ has not yet been found in the IR spectra of interstellar ices. The reason for this non-detection could be, again, that ozone's abundance is lowered by reaction of $O_3$ with $HSO_3^-$, the latter being made by the slow reaction of $H_2O$ with $SO_2$ in interstellar ice-grain mantles. These reactions might also help to explain the low abundance of sulfur-containing molecules observed in interstellar ices since the expected sulfur oxyanion products have their strongest IR features in a region obscured by interstellar silicates, near $\lambda = 10\,\mu$m. We have not yet explored these possibilities.

## 5. CONCLUSIONS

Here, we have shown that the $H_2O + SO_2 + O_3$ reaction occurs on laboratory timescales at temperatures relevant to Ganymede, Callisto, and Europa. Therefore, this reaction may explain the lack of an $O_3$ detection on Callisto, as well as ozone's spatial distribution of $SO_2$. The detection of $O_3$ on the trailing side of Ganymede, also suggests that $SO_2$ would more likely be found on that world's leading hemisphere, yet future measurements on the spatial distribution are needed to confirm this. In addition to the icy satellites, our new results may also have implications for comets and interstellar ices, where the abundance of sulfur-containing molecules is lower than expected and ozone has yet to be detected.

In the future, we will determine the reactivity of $O_3$ with other molecules under relevant conditions as we have done for $H_2O_2$ (Loeffler & Hudson 2015). Such reactions could provide a viable explanation for why $O_3$ has not been detected on more icy objects. Finally, we point out that the types of reactions presented here will not necessarily be confined to icy surfaces but could also take place in sub-surface regions, serving as a thermally driven source of both $O_2$ and $HSO_4^-$ for the Jovian icy satellites and other objects.

This work was supported by NASA's Outer Planets Research Program and the NASA Astrobiology Institute's Goddard Center for Astrobiology.

## REFERENCES

Baragiola, R. A., Atteberry, C. L., Bahr, D. A., et al. 1999, NIMPB, 157, 233
Bieler, A., Altwegg, K., Balsiger, H., et al. 2015, Natur, 526, 678
Calvin, W. M., Johnson, R. E., & Spencer, J. R. 1996, GeoRL, 23, 673
Carlson, R. W., Anderson, M. S., Johnson, R. E., et al. 1999, Sci, 283, 2062
Cooper, J. F., Johnson, R. E., Mauk, B. H., Garrett, H. B., & Gehrels, N. 2001, Icar, 149, 133
Domingue, D. L., & Lane, A. L. 1998, GeoRL, 25, 4421
Domingue, D. L., Lane, A. L., & Beyer, R. A. 1998, GeoRL, 25, 3117
Erickson, R. E., Yates, L. M., Clark, R. L., et al. 1977, AtmEn (1967), 11, 813
Famá, M., Bahr, D. A., Teolis, B. D., et al. 2002, NIMPB, 193, 775
Flynn, J. H., & Wall, L. A. 1966, JPoSL, 4, 323
Hansen, G. B., & McCord, T. 2008, GeoRL, 35, L01202
Hendrix, A. R., Cassidy, T. A., Johnson, R. E., et al. 2011, Icar, 212, 736
Hendrix, A. R., & Johnson, R. E. 2008, ApJ, 687, 706
Hibbitts, C. A., McCord, T. B., & Hansen, G. B. 2000, JGR, 105, 22541
Hoffmann, M. R. 1986, AtmEn (1967), 20, 1145
Johnson, R. E., Carlson, R. W., Cooper, J. F., et al. 2004, in Jupiter: The Planet, Satellites and Magnetosphere, ed. F. Bagenal, T. Dowling, & W. B. McKinnon (Cambridge: Cambridge Univ. Press), 485
Lacombe, S., Cemic, F., Jacobi, K., et al. 1997, PhRvL, 79, 1146
Lane, A. L., Nelson, R. M., & Matson, D. L. 1981, Natur, 292, 38
Loeffler, M. J., & Hudson, R. L. 2010, GeoRL, 37, 19201
Loeffler, M. J., & Hudson, R. L. 2013, Icar, 224, 257
Loeffler, M. J., & Hudson, R. L. 2015, AsBio, 6, 453
Loeffler, M. J., Hudson, R. L., Moore, M. H., et al. 2011, Icar, 215, 370
Lorentz, H. A. 1880, Wiedem Ann, 9, 641
Lorenz, L. 1881, Wiedem Ann, 11, 70
Maryott, A. A., & Buckley, F. 1953, Table of Dielectric Constants and Electric Dipole Moments of Substances in the Gaseous State, National Bureau of Standards Circular 537 (Gaithersburg, MD: NIST)
McCord, T. B., Hansen, G. B., Clark, R. N., et al. 1998a, JGR, 103, 8603
McCord, T. B., Hansen, G. B., Fanale, F. P., et al. 1998b, Sci, 280, 1242
Noll, K. S., Johnson, R. E., Lane, A. L., et al. 1996, Sci, 273, 341
Noll, K. S., Roush, T. L., Cruikshank, D. P., et al. 1997, Natur, 388, 45
Ozawa, T. 1965, B. Chem. Soc. Jpn., 38, 1881
Penkett, S. A., Jones, B. M. R., Brich, K. A., et al. 1979, AtmEn (1967), 13, 123
Spencer, J. R., & Calvin, W. M. 2002, AJ, 124, 3400
Spencer, J. R., Calvin, W. M., & Person, M. J. 1995, JGR, 100, 19049
Streng, A. G., & Grosse, A. V. 1959, JAChS, 81, 805
Taesler, I., & Olovsson, I. 1968, Acta Crystallogr., B24, 299
Vyazovkin, S. 1996, Int. J. Chem. Kinet., 28, 95
Vyazovkin, S., & Wight, C. A. 1997, ARPC, 48, 125
Walrafen, G. E., & Dodd, D. M. 1961, Trans. Faraday Soc., 57, 1286